Int. J. Heat Mass Transfer. Vol. 34, No. 10, pp. 2521–2534, 1991
Printed in Great Britain

0017–9310/91 $3.00 + 0.00

Determination of wave-induced fluctuations of wall temperature and convection heat transfer coefficient in the heating of a turbulent falling liquid film

T. H. LYU and I. MUDAWAR
Boiling and Two-phase Flow Laboratory, School of Mechanical Engineering,
Purdue University, West Lafayette, IN 47907, U.S.A.

(*Received* 10 *July* 1990 *and in final form* 15 *November* 1990)

Abstract—This study examines the transient thermal response of a vertical electrically-heated wall during sensible heating of a turbulent wavy film. It is shown how the wall temperature can be decomposed into two components. The first is steady and accounts for the stream-wise increase in the wall and film temperatures, and the second is periodic and corresponds to temperature fluctuations due to the film waviness. By assuming periodicity in the wall temperature fluctuation in response to large film waves, the second component is solved numerically using liquid temperature data measured across the film to define the boundary condition at the wall–liquid interface. Results show that, during the period of a large wave, the wall temperature is fairly uniform but the convection heat transfer coefficient undergoes significant fluctuation. The fluctuation amplitude of the latter decreased with increasing film Reynolds number.

1. INTRODUCTION

THE ABILITY to produce high rates of heat removal with minimal pumping power lends the utility of falling film flow to a large variety of thermal and chemical process equipment. Industrial needs in the areas of design and performance assessment of these equipment have triggered extensive research aimed at developing a good understanding of the transport phenomena associated with a falling liquid film. Spanning over seven decades of aggressive research, the task of accurately predicting film behavior remains a difficult one largely because of the effects of turbulence and film waviness [1].

Several studies have shown periodic changes in the transport characteristics of liquid films caused by interfacial waves. Examples of these studies include measurements of fluctuations in wall shear stress [2] and mass transfer rate [3]. Ganchev and Trishin [4] measured the influence of waviness on heat transfer to a falling water film by a single thermocouple positioned within the film. They detected a sharp drop in liquid temperature when the crest of a large wave approached the thermocouple bead. The temperature then increased until the advent of the next large wave.

The periodic fluctuation of liquid temperature is a unique feature which distinguishes wave film flows from most types of internal or external boundary-layer flows. Interfacial waves affect the flow field, substrate thickness, and turbulent intensity in the film. Therefore, both the liquid temperature and convection heat transfer coefficient at the wall, as well as wall temperature, would fluctuate in response to these waves. Understanding and characterizing these fluctuations within a wave period is of paramount importance to the development of accurate heat transfer models and useful correlations.

The present study introduces the experimental techniques used for the simultaneous measurements of film thickness, wall temperature, liquid temperature profile and wave velocity. Presented is a numerical approach to modelling heat transfer from an electrically-heated wall to a falling liquid film based upon the assumption of periodicity in the temperature fluctuations. Instantaneous temperature profile measurements obtained within the film are used as boundary conditions at the wall–liquid interface, allowing the model to determine the fluctuations of wall temperature and convective heat transfer coefficient over a wave period. These results are used to point out how interfacial waves can induce large periodic changes in heat transfer for certain film conditions and negligible changes for others. The fundamental and practical implications of these findings are also discussed.

2. EXPERIMENTAL METHODS

As shown in Fig. 1, a liquid film was formed by supplying water from the inside of a tubular porous tube and allowing the water to fall freely on the outside of a 25.4 mm diameter vertical test section attached to the lower end of the porous tube. Details of the external flow loop are available in a previous paper [5]. The test section was constructed from a 757 mm long fiberglass plastic rod followed by a 781 mm long stainless steel tube having a thickness of 0.41 mm. A d.c. current reaching values as high as 750 A

NOMENCLATURE

c_p	specific heat at constant pressure
h	convection heat transfer coefficient
h^*	dimensionless convection heat transfer coefficient, $hv_f^{(2/3)}/k_f g^{1/3}$
k	thermal conductivity
L	heated section wall thickness
Pr	liquid Prandtl number
q	heat flux
$\bar{q}$	time average of heat flux, $\dot{q}L$
$\dot{q}$	volumetric rate of heat generation
Re	Reynolds number, $4\Gamma/\mu_f$
t	time
T	temperature
$\bar{u}$	mean film velocity
V_w	wave velocity
x_p	longitudinal distance from the leading edge of the heated section
y	distance from the inner surface of the wall in the stationary coordinate system
x, y, t	stationary coordinates.

Greek symbols

Γ	mass flow rate per unit film width
δ	film thickness
δ_{buf}	buffer sublayer thickness
δ_{lam}	laminar sublayer thickness
ζ	moving (wave) coordinate
η	distance from inner solid wall in the moving (wave) coordinate system
λ	wavelength
μ	dynamic viscosity
ν	kinematic viscosity
ξ	distance from the solid wall
ρ	density
τ	'time' in moving (wave) coordinate system
τ_w	wave period
Φ	coordinate transformation.

Subscripts

f	fluid
m	average value; time mean
max	maximum
min	minimum
s	solid
w	wall
δ	film free interface.

Superscript

$\bar{}$	average value.

at 15 V was supplied through the stainless steel section producing the required heat flux to the film. The heated tube was insulated on the inside with a Delin rod which maintained a thin circumferential air gap with the inner tube wall by 17 pairs of nylon screws spring loaded between the rod and the wall of the stainless steel tube. A thermocouple made from 0.127 mm copper and constantan wire was embedded in a small mass of thermally conducting boron nitride epoxy which filled the tip of each screw. The epoxy was machined to the exact curvature of the inner stainless steel wall and wetted with thermally conducting silicon grease to create a smooth mating interface with the heated wall. The thermocouple pairs were mounted 180° apart in the circumferential direction to assist the operator in ensuring a circumferentially symmetrical film flow by careful alignment of the test section. The pairs were spaced closely near the leading edge of the heated section and further apart in the downstream region. The thermocouple pairs were utilized to measure the extent of the thermal entrance region and the time average values of the inner wall temperatures since their transient response to wave-induced temperature fluctuations were dampened by the thermal mass of the surrounding epoxy within the nylon screw tips.

Figure 2 shows relative positions of the film-side probes used in the present measurements: a thickness probe, a probe for calibrating the thickness probe and a series of thermocouples, all mounted on the outside of the test section in the same radial plane. Located 29.7 mm downstream from the first thickness probe was a second thickness probe which facilitated the measurement of wave velocity. A 41 deg azimuthal separation angle kept the second thickness probe outside the wakes created by the upstream probes.

The present measurements were taken with the upstream probes shown in Fig. 2 located 287 mm from the leading edge of the heated section. Present inner thermocouple measurements and previous results from ref. [5] confirmed that this measurement location was outside the thermal entrance region.

Figure 3 shows a probe assembly block made from fiberglass plastic which positioned the film-side probes across the film. The entire block was wedge-mounted on a vertical rail to facilitate vertical translation of the probes. Radial translation of the probes toward the heated wall was controlled by two micrometer translation stages attached to the vertical rail. Additional alignment of the probes with respect to the wall was achieved by a rectangular housing having six Delin-tipped stainless steel screws which prevented lateral displacement of the test section during the experiments. A third micrometer stage allowed the thickness calibration probe to be translated radially while the probe assembly block was fixed in place. It should be noted that the complex devices used in positioning the film-side probes were all essential for the delicate

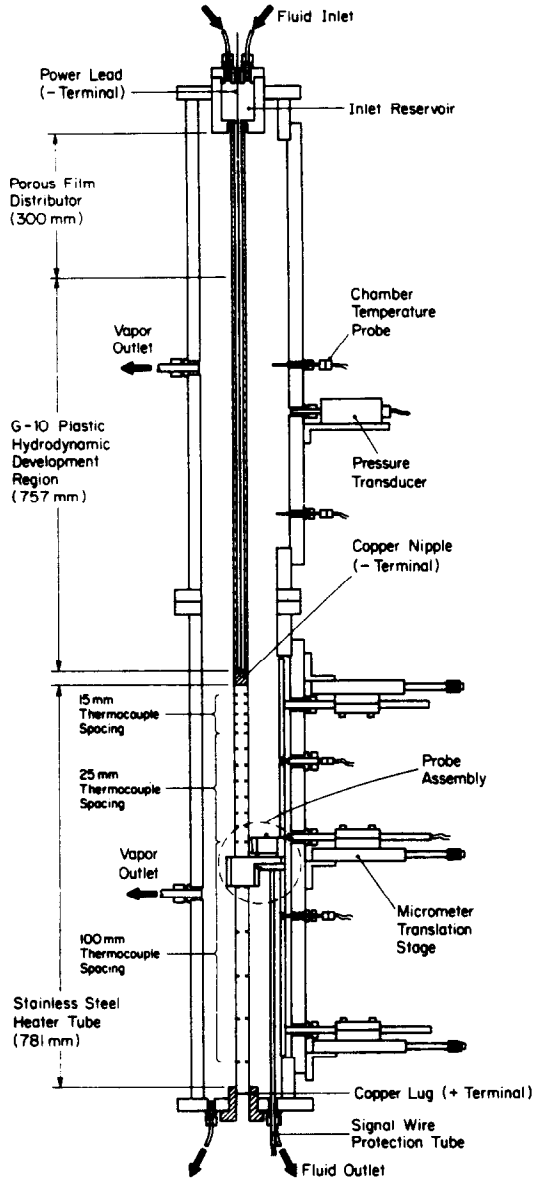

FIG. 1. Schematic diagram of the test chamber.

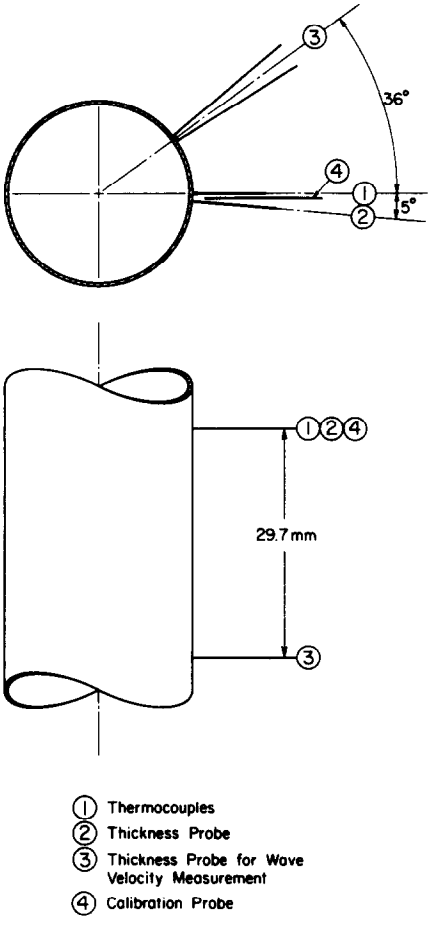

FIG. 2. Relative positions of the thickness and temperature probes.

measurements of film thickness and liquid temperature.

The instantaneous temperature profile across the liquid film was measured by twelve thermocouples made from 0.0508 mm diameter chromel and constantan wires. The thermocouples were mounted over a 5 mm span on a fiberglass plastic knife edge protruding from the probe assembly block as shown in Fig. 4. The thermocouple beads were exposed to liquid to ensure a short time constant (0.39–0.55 ms) in the response to liquid temperature fluctuations.

The thickness probe was made from a 0.0254 mm diameter platinum–10% rhodium wire having a relatively large temperature coefficient of resistivity. The thickness was determined from the voltage drop across the probe leads in response to a constant d.c. current. The large temperature difference between the portions of wire in the liquid and in the gas caused large changes in the total wire resistance in response to changes in the length of wire in each medium. Theoretically, the relationship between film thickness and voltage drop is linear, however extensive calibration was required prior to each experiment. The calibration was performed with the heater power turned on in order to duplicate the conditions of each experiment while accounting for the sensitivity of the probe electrical resistance to temperature changes across the film. The calibration technique involved positioning the thickness probe across the film and translating the calibration probe, which is similar in construction to the thickness probe, radially towards the film free interface. Contact between the tip of the calibration probe and the film interface triggered surges in the calibration probe signal. At each known distance of the calibration probe from the wall, the contact times identified calibration points on a thickness probe time record which was measured simultaneously with the calibration probe record. The measurement resolution and response time of the thickness probe were estimated to be 0.05 mm and

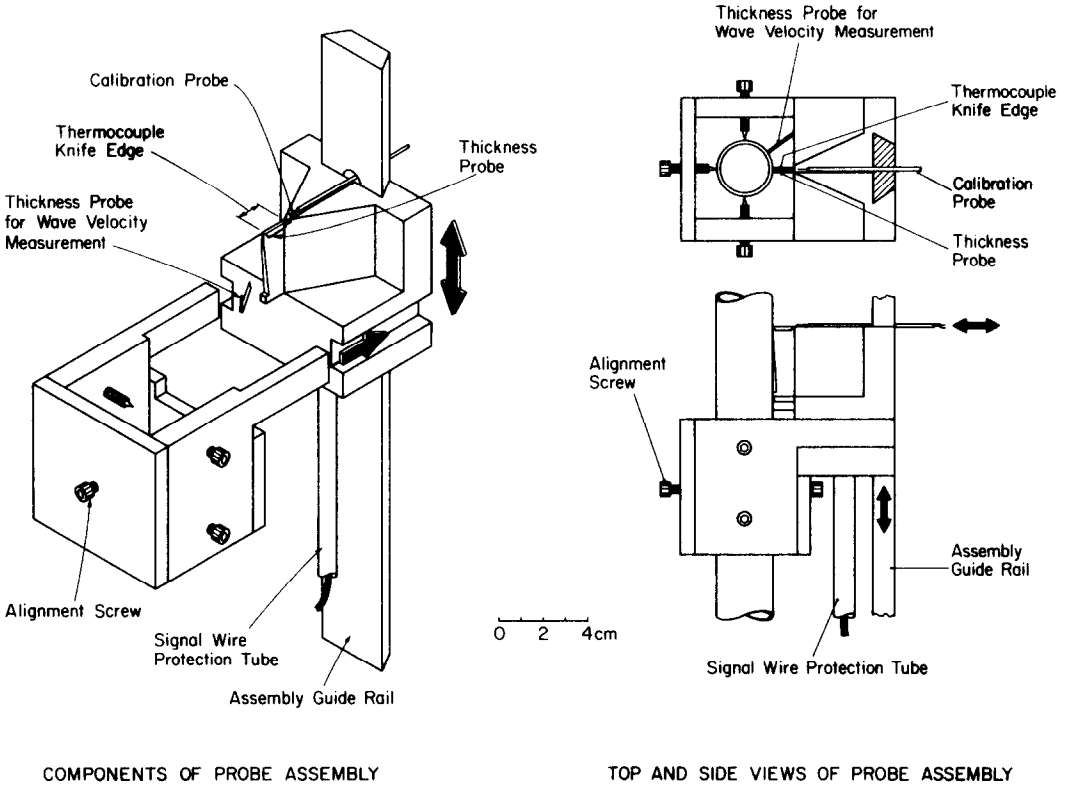

FIG. 3. Probe assembly block.

0.14 ms, respectively. Data were measured with the aid of a high speed Keithley 500 data acquisition and control system coupled to a Compaq 386-40 microcomputer. Liquid temperature and film thickness data were sampled at a frequency of 400 or 500 Hz over periods ranging from 1 to 5 s.

3. EXPERIMENTAL RESULTS

The local temperature profile within the film was measured by a maximum of twelve thermocouples, Fig. 4, for film flow rates in the range $2700 \leqslant Re \leqslant 11\,700$ and heat fluxes ranging from 0 to 75 000 W m^{-2}. Figure 5 shows time records of liquid temperature obtained by the thermocouple closest to the wall. Also shown are thickness records measured during the same period. The records display fairly periodic fluctuations in temperature and thickness marred by occasional irregularities as shown in Fig. 5(a). Liquid temperature increased in the thin substrate regions separating the large waves and decreased sharply in the wave crest region. This trend is consistent with the findings of Ganchev and Trishin [4].

The periodicity in temperature profile changes within a wave is displayed in Fig. 6. The profile tends to retain its character at the beginning and end of a wave period. The three cases shown in Fig. 6 are for individual waves at the conditions indicated rather than averages of profiles for a series of waves in each data record.

Since periodicity cannot be ascertained by examining an individual wave period, statistical analysis was performed on the entire data base obtained in the present study. Cross-covariance between the liquid temperature and film thickness signals was strong for $Re < 10\,000$ and $\bar{q} > 10\,000$ W m^{-2} and revealed only a slight phase shift between the two signals caused by temperature excursions associated with relative liquid motion between the substrate and the large wave. Cross-spectral analysis showed a distinct band of dominant frequencies in the relationship between the two signals. Details of these statistical findings can be found elsewhere [6].

Wave velocity was determined for each test by dividing the distance between the upstream and downstream thickness probes, Fig. 2, by the average time difference between two corresponding large wave peaks traced on the time records of two thickness probes as shown in Fig. 7. The results of limited wave velocity measurements used in the present numerical analysis are shown in Table 1 along with previous measurements by Chu and Dukler [7] and Takahama and Kato [8].

4. MODEL DEVELOPMENT

The instantaneous convection heat transfer coefficient in the present study is defined with respect

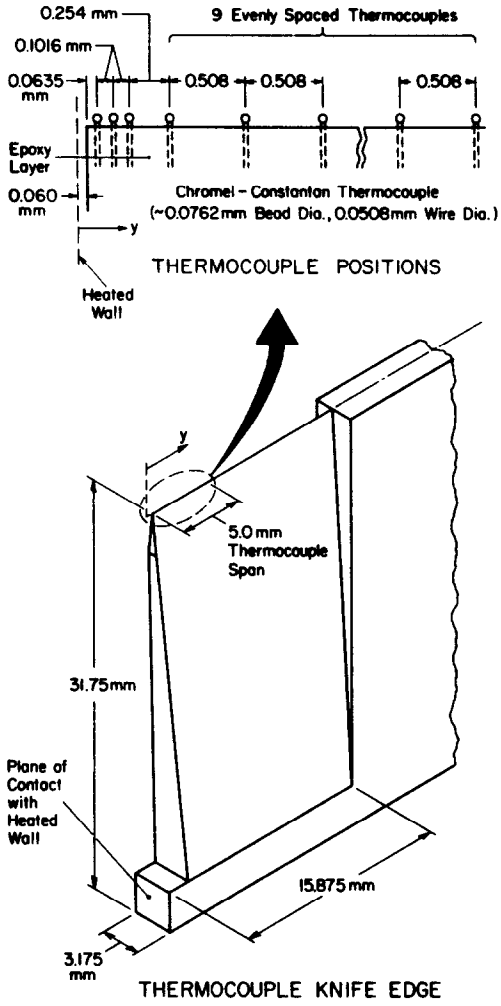

FIG. 4. Thermocouple positions on the thermocouple knife edge.

to the instantaneous values of heat flux q and wall temperature T_w

$$h \equiv \frac{q}{T_w - T_{f,m}} \tag{1}$$

where $T_{f,m}$ is the mean liquid temperature at a stream-wise distance x_p from the leading edge of the heated test section based upon energy conservation for steady flow of a smooth liquid film falling on a uniformly heated wall

$$T_{f,m}(x_p) = T_{f,m}(x_p = 0) + \frac{\bar{q}}{\rho_f c_{p,f} \Gamma} x_p \tag{2}$$

where $\bar{q}$ is the time average value of q determined from electrical measurement across the ends of the stainless steel heated tube. The conventional definition of mean liquid temperature (i.e. bulk temperature or mixing cup temperature) commonly employed in defining the heat transfer coefficient for internal flows could not be used in the present study because the velocity distribution across the film was not measured simultaneously with liquid temperature and film thickness. Furthermore, the definition of h given in equation (1) facilitates the determination of transient variables at the wall with respect to a pre-determined value for bulk liquid temperature independent of time.

A two-dimensional transient conduction problem involving a periodic boundary disturbance is considered in determining the wall temperature and convection heat transfer coefficient variations with respect to time in stationary coordinates, as shown in Fig. 8(a), where the origin of the coordinate system is positioned at the inner side of the wall at a distance x_p from the leading edge of the heated wall. The governing energy equation for a heat generating wall with constant properties is

$$\rho_s c_{p,s} \frac{\partial T}{\partial t} = k_s \left(\frac{\partial^2 T}{\partial x^2} + \frac{\partial^2 T}{\partial y^2} \right) + \dot{q} \tag{3}$$

where $\dot{q}$ is a constant rate of heat generation per unit volume (i.e. $\dot{q} = \bar{q}/L$). The boundary conditions for equation (3) corresponding to $y = 0$ and L are respectively

$$-k_s \left. \frac{\partial T}{\partial y} \right|_{y=0} = 0 \tag{4}$$

$$-k_s \left. \frac{\partial T}{\partial y} \right|_{y=L} = -k_f \left. \frac{\partial T_f}{\partial y} \right|_{y=L}. \tag{5}$$

The present analysis is based on the assumption that the film thickness and *fluctuating* component of liquid temperature at a fixed distance from the wall are both *periodic and possess similar frequencies* at any stream-wise distance x_p from the leading edge of the heated wall, as was demonstrated by the experimental results and statistical analyses discussed in the previous section. Although the thickness and liquid temperature *fluctuation* are fairly periodic, the temperature variations of the wall and the film with x_p are not. This renders the heat transfer problem fundamentally different from the hydrodynamic problem, which is periodic along the heater length assuming liquid properties independent of temperature. The time average wall temperature, $\bar{T}(x_p, y)$, and mean liquid temperature increase with increasing x_p. In the thermally developed region, energy conservation requires that both temperatures increase linearly with x_p. Experimental data from thermocouples attached to the inner wall of the heater ($y = 0$) confirmed the linearity of the relationship between wall temperature $\bar{T}(x_p, 0)$ and x_p with less than a 7% error in the thermally developed region. Based on this observation, wall temperature $T(x, y, t)$ can be decomposed into two components: one, $T_1(x)$, which is steady and increases linearly with longitudinal distance, and the other, $T_2(x, y, t)$, which is periodic. Then

$$T(x, y, t) = T_1(x) + T_2(x, y, t). \tag{6}$$

Over one wavelength λ, $T_1(x)$ satisfies the equation

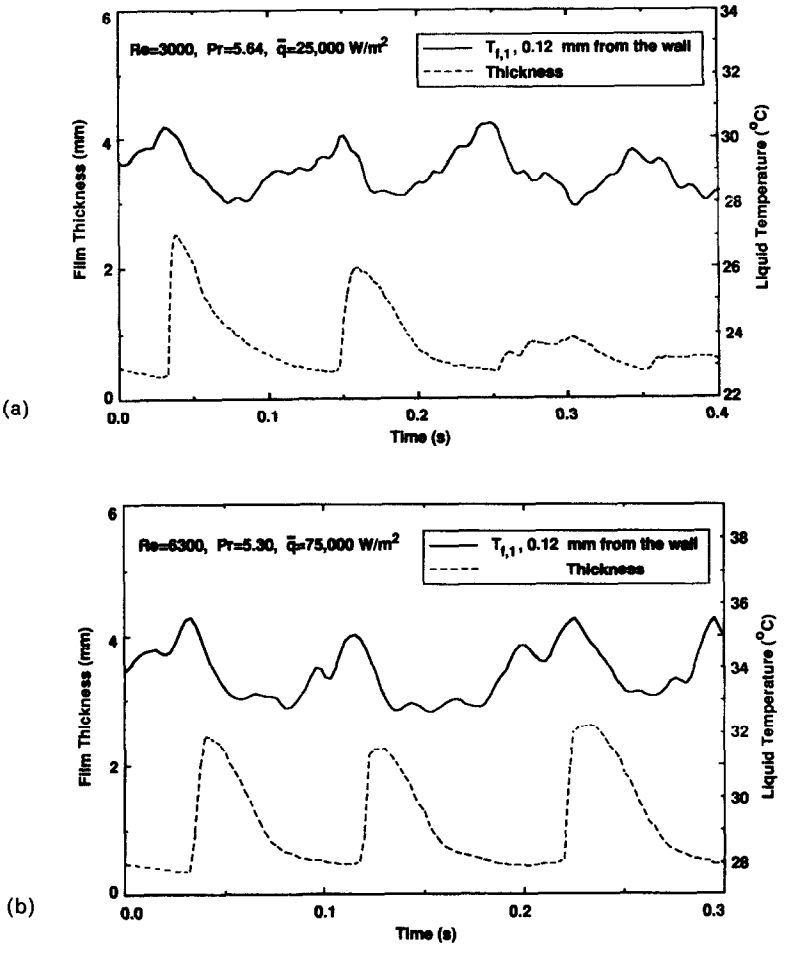

FIG. 5. Time records for film thickness and liquid temperature for: (a) $Re = 3000$, $\bar{q} = 25\,000$ W m^{-2}; (b) $Re = 6300$, $\bar{q} = 75\,000$ W m^{-2}.

$$\frac{d^2T_1}{dx^2} = 0 \tag{7}$$

which in turn satisfies the condition

$$\left.\frac{dT_1}{dx}\right|_{x=\lambda} = \left.\frac{dT_1}{dx}\right|_{x=0}. \tag{8}$$

The periodic component $T_2(x, y, t)$ satisfies the differential equation

$$\rho_s c_{p,s}\frac{\partial T_2}{\partial t} = k_s\left(\frac{\partial^2 T_2}{\partial x^2} + \frac{\partial^2 T_2}{\partial y^2}\right) + \dot{q} \tag{9}$$

and the boundary conditions

$$T_2(\lambda, y, t) = T_2(0, y, t) \tag{10}$$

$$\left.\frac{\partial T_2}{\partial x}\right|_{x=\lambda} = \left.\frac{\partial T_2}{\partial x}\right|_{x=0} \tag{11}$$

$$-k_s\left.\frac{\partial T_2}{\partial y}\right|_{y=0} = 0 \tag{12}$$

$$-k_s\left.\frac{\partial T_2}{\partial y}\right|_{y=L} = -k_f\left.\frac{\partial T_f}{\partial y}\right|_{y=L}. \tag{13}$$

It should be noted that the boundary conditions for $T(x, y, t)$ corresponding to $x = 0$ and λ are

$$\begin{aligned} T(\lambda, y, t) &= T_1(\lambda) + T_2(\lambda, y, t) \\ &= T_1(0) + \int_0^\lambda \frac{dT_1}{dx}dx + T_2(0, y, t) \\ &= T(0, y, t) + \int_0^\lambda \frac{dT_1}{dx}dx \end{aligned} \tag{14}$$

and

$$\left.\frac{\partial T}{\partial x}\right|_{x=\lambda} = \left.\frac{dT_1}{dx}\right|_{x=\lambda} + \left.\frac{\partial T_2}{\partial x}\right|_{x=\lambda} = \left.\frac{dT_1}{dx}\right|_{x=0} + \left.\frac{\partial T_2}{\partial x}\right|_{x=0} = \left.\frac{\partial T}{\partial x}\right|_{x=0}. \tag{15}$$

It is well known that a periodic problem in one

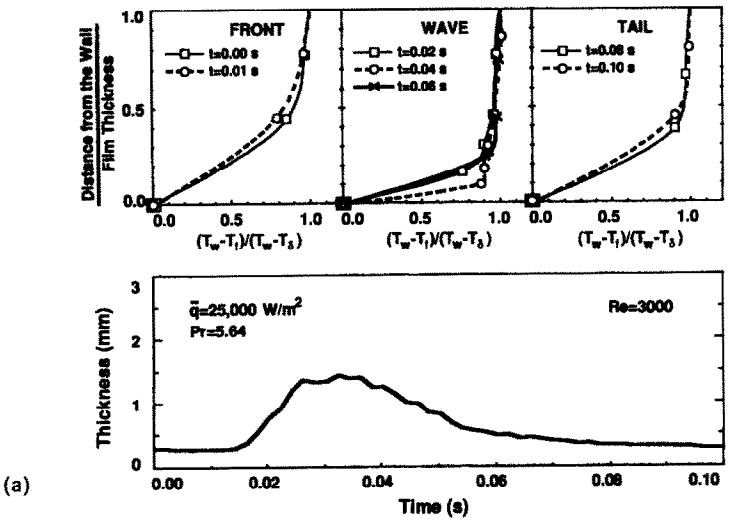

(a)

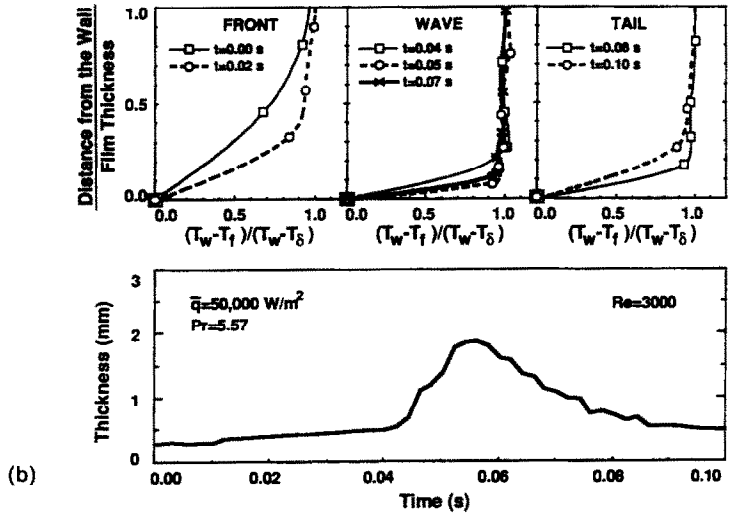

(b)

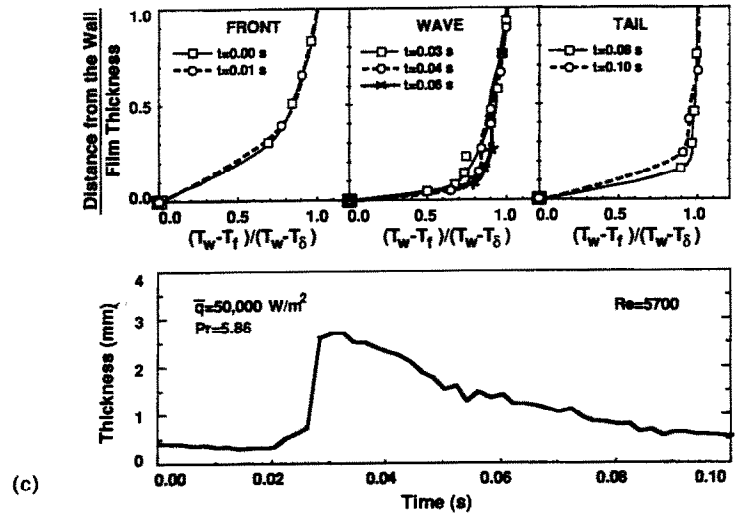

(c)

FIG. 6. Temperature profiles at different times within a wave for: (a) $Re = 3000$, $\bar{q} = 25\,000$ W m^{-2}; (b) $Re = 3000$, $\bar{q} = 50\,000$ W m^{-2}; (c) $Re = 5700$, $\bar{q} = 50\,000$ W m^{-2}. The total time shown for each case is not exactly equal to the period of the corresponding wave.

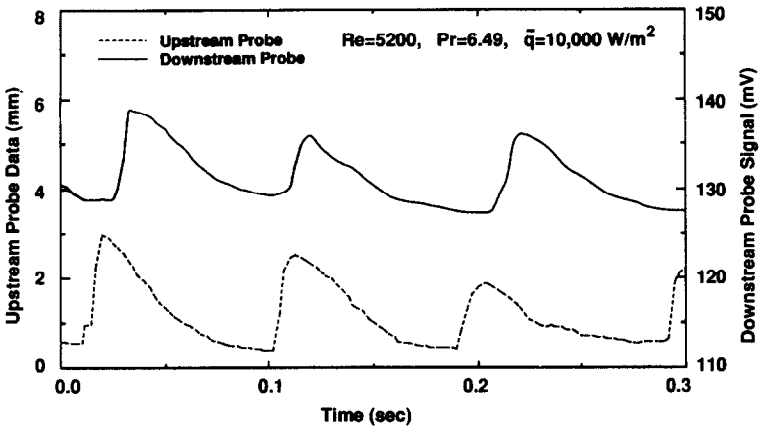

FIG. 7. Time records from the two thickness probes used in the determination of wave velocity.

Table 1. Wave velocity data

				Present study $x = 1.04$ m		Takahama and Kato (1980) $x = 1.50$ m		Chu and Dukler (1975) $x = 4.17$ m	
Γ (kg m^{-1} s^{-1})	Re	Pr	$\bar{q}$ (W m^{-2})	V_w (m s^{-1})	$V_w/\bar{u}$	V_w (m s^{-1})	$V_w/\bar{u}$	V_w (m s^{-1})	$V_w/\bar{u}$
1.22	6000	5.53	75000	1.87	1.43				
1.22	5200	6.49	10000	1.88	1.40				
	5000	7.53	0			1.85	1.30		
	5000		0					2.18	1.25
1.83	8800	5.67	75000	2.06	1.43				
1.83	7700	6.59	10000	2.05	1.38				
	7500	7.53	0			2.10	1.25		
	7500		0					2.55	1.10

coordinate system can sometimes be solved as a steady-state problem in another coordinate system. In the present model, $T_2(x, y, t)$ will be determined in moving wave coordinates, where the solid wall is viewed as moving upward at a constant speed V_w equal to the speed of the wave as shown in Fig. 8(b). The original differential equation for $T_2(x, y, t)$ is transformed from stationary physical coordinates (x, y, t) to the computational moving coordinates (ζ, η, τ) by applying the chain rule for differentiation. The coordinates are transformed according to a transformation, Φ, defined as

$$(x, y, t) \rightarrow (\zeta, \eta, \tau) = (x - V_w t, y, t). \tag{16}$$

The definition of ζ given in equation (16) facilitates solving for temperature with respect to x at a given time, or with respect to t at a given value of x. The former is used here because the present analysis is based on the assumption of a periodic film motion in waves having a uniform wavelength $\lambda = V_w \tau_w$ as shown in Fig. 8, τ_w being the period of the temperature (or thickness) time record.

Now a new variable $\theta(\zeta, \eta, \tau)$ is defined as

$$\theta(\zeta, \eta, \tau) = \theta[\Phi(x, y, t)] = T_2[\Phi^{-1}\Phi(\zeta, \eta, \tau)] = T_2(x, y, t). \tag{17}$$

The differentiation chain rule gives

$$\frac{\partial T_2}{\partial t} = \frac{\partial \theta}{\partial t} = \frac{\partial \theta}{\partial \tau} - V_w \frac{\partial \theta}{\partial \zeta} \tag{18}$$

$$\frac{\partial T_2}{\partial x} = \frac{\partial \theta}{\partial x} = \frac{\partial \theta}{\partial \zeta} \tag{19}$$

$$\frac{\partial T_2}{\partial y} = \frac{\partial \theta}{\partial y} = \frac{\partial \theta}{\partial \eta} \tag{20}$$

from which it is also found that

$$\frac{\partial^2 T_2}{\partial x^2} = \frac{\partial^2 \theta}{\partial x^2} = \frac{\partial^2 \theta}{\partial \zeta^2} \tag{21}$$

$$\frac{\partial^2 T_2}{\partial y^2} = \frac{\partial^2 \theta}{\partial y^2} = \frac{\partial^2 \theta}{\partial \eta^2}. \tag{22}$$

Substituting the above results into equation (9) yields the differential equation

$$\rho_s c_{p,s} \frac{\partial \theta}{\partial \tau} - \rho_s c_{p,s} V_w \frac{\partial \theta}{\partial \zeta} = k_s \frac{\partial^2 \theta}{\partial \zeta^2} + k_s \frac{\partial^2 \theta}{\partial \eta^2} + \dot{q}. \tag{23}$$

From equation (12), the boundary condition for

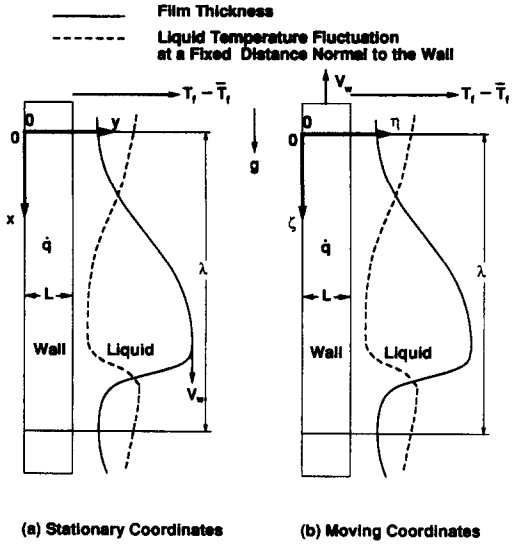

FIG. 8. Schematic representation of thickness and liquid temperature fluctuations of a liquid film falling on an electrically heated wall in: (a) stationary coordinates; (b) moving coordinates.

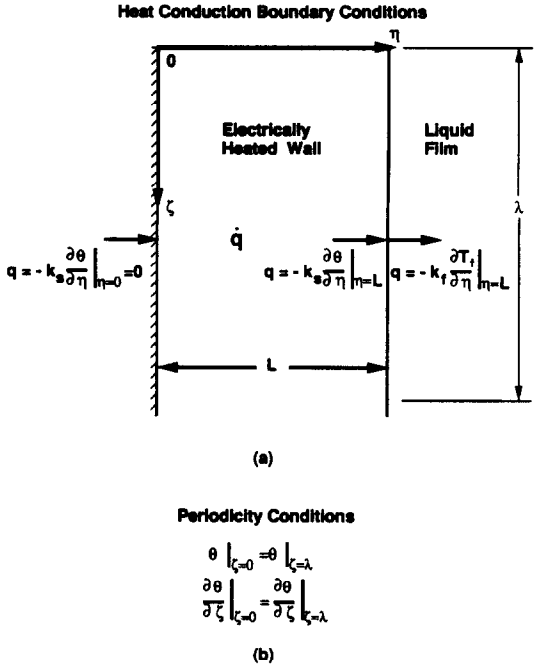

FIG. 9. Boundary conditions for the heated wall over one wavelength.

$\theta(\zeta, \eta, \tau)$ at $\eta = 0$ becomes

$$\frac{\partial \theta}{\partial \eta} = 0 \quad \text{at } \eta = 0 \tag{24}$$

and the boundary condition for T_2 at $y = L$, equation (13), results in

$$-k_s \frac{\partial \theta}{\partial \eta}\bigg|_{\eta=L} = -k_s \frac{\partial T_2}{\partial y}\bigg|_{y=L} = -k_s \frac{\partial T_f}{\partial y}\bigg|_{y=L}. \tag{25}$$

The periodic conditions for T_2, equations (10) and (11), result in the following boundary conditions for θ:

$$\theta(\lambda, \eta, \tau) = \theta(0, \eta, \tau) \tag{26}$$

$$\frac{\partial \theta}{\partial \zeta}\bigg|_{\zeta=0} = \frac{\partial \theta}{\partial \zeta}\bigg|_{\zeta=\lambda} \tag{27}$$

as illustrated in Fig. 9.

In moving coordinates, the film thickness and liquid temperature profile remain fixed as the solid wall is being drawn upward at a constant speed V_w. The boundary conditions given in equations (24)–(27) point to a steady solution for θ in moving coordinates since $\partial T_f/\partial \eta|_{\eta=L}$ is independent of τ. It is important to note that the boundary condition at $\eta = L$ not only defines the temperature gradient at that boundary but it also assigns temperature values. Therefore, $\theta(\zeta, \eta, \tau)$ can be simplified as $\theta(\zeta, \eta)$ which satisfies the steady-state elliptic equation

$$-\rho_s c_{p,s} V_w \frac{\partial \theta}{\partial \zeta} = k_s \frac{\partial^2 \theta}{\partial \zeta^2} + k_s \frac{\partial^2 \theta}{\partial \eta^2} + \dot{q}. \tag{28}$$

5. CALCULATION PROCEDURE

Equation (28) was solved using the SIMPLER algorithm [9]. The boundary condition at $\eta = L$, equation (25), was determined from the liquid temperatures $T_{f,i}$ measured by thermocouples positioned in liquid, at distances ξ_i from the wall ($i = 1$–12) as shown in Fig. 4. In order to simplify the calculations, T_1 was set to zero at $x = 0$ where the liquid temperatures $T_{f,i}(t)$ were measured. This facilitated using the measured liquid temperatures themselves instead of corrected temperatures, $T_{f,i} - T_1(0)$, as boundary conditions in solving for θ. Unfortunately, the temperature measurements corresponding to $i = 3$–12 were intermittent due to periodic penetrations of the thermocouple beads outside the free liquid film interface. Therefore, the heat flux was calculated using a second-order polynomial curve fit based on $T_{f,1}$, $T_{f,2}$ and T_w, where the unknown wall temperature T_w is equal to $\theta(\zeta, L)$ since $T_1(0) = 0$. The actual value of T_w was determined from the numerical solution. The boundary condition given in equation (25) was expressed as

$$q = -k_s \frac{\partial \theta}{\partial \eta}\bigg|_{\eta=L} = -k_f \frac{\partial T_f}{\partial y}\bigg|_{y=L} = -k_f \frac{\dfrac{\xi_2}{\xi_1}(T_{f,1} - T_w) - \dfrac{\xi_1}{\xi_2}(T_{f,2} - T_w)}{\xi_2 - \xi_1}. \tag{29}$$

Assuming the protruded side of the thermocouple knife edge, Fig. 4, maintains perfect contact with the heated wall, the theoretical values of ξ_1 and ξ_2 are 0.12

and 0.22 mm. Maintaining these distances required extreme care in positioning the probe assembly block shown in Fig. 3 as discussed previously.

One concern in the determination of the boundary condition at $\eta = L$ was the feasibility of calculating the temperature gradient with sufficient accuracy based on T_w and measured temperatures $T_{f,1}$ and $T_{f,2}$. It is especially important to know whether the gradient undergoes large variations between the wall and the first thermocouple. In the viscous sublayer of a turbulent boundary layer, the temperature gradient is constant and the fluid temperature can be assumed to vary linearly with the distance from the wall. Outside the viscous sublayer the temperature gradient begins to change with distance. It is difficult to determine the extent of the viscous sublayer in a turbulent falling film due to a lack of knowledge of the hydrodynamic structure of the film in the presence of interfacial waves. However, using the law-of-the-wall turbulent boundary layer profile, the outer edges of the viscous and buffer sublayers within a smooth film can be approximated, respectively, as (see ref. [10])

$$\delta_{lam} = \frac{5\nu_f}{\sqrt{(g\delta)}} \tag{30}$$

$$\delta_{buf} = \frac{30\nu_f}{\sqrt{(g\delta)}} \tag{31}$$

where

$$\delta = 0.136\, Re^{0.583}\left(\frac{\nu_f^2}{g}\right)^{1/3}. \tag{32}$$

For the conditions of the present study, equations (30) and (31), predict values of δ_{lam} and δ_{buf} equal to 0.06 and 0.36 mm, respectively. This first-order approximation shows that the first thermocouple is generally located outside the laminar sublayer but within the inner 20% extent of the buffer sublayer. Thus, some non-linearity is expected in the liquid temperature profile between the wall and the first thermocouple. This non-linearity is corrected by the polynomial curve fit to $T_{f,1}$ and $T_{f,2}$.

In reality, the temperature profile undergoes significant changes during a wave period. As shown in Fig. 6, the profile is fairly linear or parabolic in the thin substrate regions upstream and downstream from the large wave. The temperature gradient becomes steeper within the large wave but is still predictable based upon measurements obtained with the two thermocouples closest to the wall.

Wavelength λ was determined as the product of wave velocity, obtained from thickness measurements, and wave period. The wave period was calculated by multiplying the data sampling time interval by the number of $T_{f,1}$ data required to meet the periodic condition for a single wave. The ranges of wave velocity and wavelength used were $1.2\ \text{m s}^{-1} \leqslant V_w \leqslant 2.4\ \text{m s}^{-1}$ and $0.17\ \text{m} \leqslant \lambda \leqslant 0.35\ \text{m}$, respectively. Although the wave period could be easily determined with good accuracy, wave velocity was difficult to determine accurately since its measurement resolution was limited to $\pm 0.2\ \text{m s}^{-1}$.

After determining the wavelength λ for each set of operating conditions, the wave velocity in the term on the left-hand side of equation (28) was perturbed *numerically* to determine the effect of this term on the thermal response of the wall. Wave velocity was found to have a negligible effect on T_w and h, less than 0.1% in the range 0.1–$5.4\ \text{m s}^{-1}$, and a significant effect for velocities below $0.1\ \text{m s}^{-1}$. Physically, this implies that the penetration distance of the wall temperature fluctuation in response to the passage of a series of large waves of a given wavelength is small unless the waves move very slowly (i.e. the wave period is very large). For most conditions of practical interest, the wall responds to the wave more by convecting its energy to the film than by incurring temperature fluctuation due to thermal storage. Only under the extreme condition of very low wave velocity is the effect of the waves felt deep inside the wall, causing relatively large fluctuations in the wall temperature. It should be noted that, despite the insensitivity of the calculated wall temperature and convection heat transfer coefficient to relatively large perturbations in the magnitude of V_w, the effect of waviness on the heat transfer to the film is still implicit in the boundary condition between the wall and the film, equation (25), instead of the convection term in equation (28).

6. RESULTS AND DISCUSSION

Wall temperature fluctuations were found to be small compared with the changes in liquid temperature. Table 2 shows different operating conditions and parameters used in the present numerical analysis. The maximum amplitudes are defined as $(\Delta T_w)_{max} = T_{w,max} - T_{w,min}$ and $(\Delta T_f)_{max} = T_{f,max} - T_{f,min}$ corresponding to measurements obtained by the first thermocouple. The present results show that the wall temperature can be assumed constant without sacrificing accuracy in calculating h despite the small thermal capacitance of the wall used in the tests. It is interesting to recall that the wall thickness of the test section was only 0.41 mm, which is smaller than the thickness of most surfaces used in industrial heat exchangers.

Figures 10(a)–(c) reveal that fluctuations in the local heat flux and convection heat transfer coefficient are opposite to that of liquid temperature since the wall temperature is fairly constant. The fluctuation amplitudes of q and h are very large for $Re = 3000$ and insignificant for $Re = 10\,800$. Faghri and Seban [11] reported predictions for the local heat transfer coefficient variation during the period of a *laminar sinusoidal* film wave for a constant wall temperature condition. The present results show a similar trend of decreasing amplitude of the heat transfer coefficient with increasing Reynolds number. Furthermore, both the present study and the highest Re (i.e. 472) results

of Faghri and Seban indicate that the variation of the heat transfer coefficient and thickness are essentially in phase.

As shown in Figs. 10(a)–(c), the heat transfer coefficient increases within the wave and has a maximum value in the wave back region. Brauner and Maron [3] detected a similar phenomenon in mass transfer experiments involving inclined thin film flow. Maximum mass transfer rates were found just beyond the wave peaks. Wasden and Dukler [12] showed that the velocity gradient was steep and the circulating streamlines were close to the wall in the wave back region. Therefore, stronger mixing and turbulence intensity provide a plausible explanation why the peak value of h occurs in that region.

Values of the time average convection heat transfer coefficient, $\bar{h}$, and maximum amplitude of h for all the present data records are shown in Table 2. Values of the amplitude ratio $\Delta(h/\bar{h})(=(h_{max}-h_{min})/\bar{h})$ reveal that the convection heat transfer coefficient is relatively constant at high Reynolds numbers and high heat fluxes, perhaps due to the higher levels of turbulence mixing produced at these conditions. The heat transfer coefficient also increases with increasing heat flux over the entire Re range. Also, the amplitude ratio decreases with increasing heat flux at a given flow rate for the two higher Reynolds numbers. But this trend does not hold for the lower Reynolds number. Figure 11 shows approximate correlations for $(h/\bar{h})_{max}$ and $(h/\bar{h})_{min}$ vs Reynolds number for $25\,000\ W\,m^{-2} < \bar{q} < 75\,000\ W\,m^{-2}$. It may be argued from these results that the use of empirical smooth-film turbulence models is justifiable for $Re > 10\,000$ provided these models accurately account for turbulence near the film interface.

The following empirical correlation for sensible heating of a liquid film was developed earlier [5]:

$$h^* = 0.0106 Re^{0.3} Pr^{0.63}. \quad (33)$$

Figure 12 shows the present results are in good agreement with the above correlation in the low heat flux range used in the development of equation (33). However, the present results are higher than predicted by equation (33) for fluxes in excess of $47\,000\ W\,m^{-2}$. This deviation may be evidence that the convection heat transfer coefficient of a falling film is not only a function of the Reynolds and Prandtl numbers, but may also be affected by other parameter(s) which account for the coupled effects of heat transfer and film waviness. In the absence of further evidence, one can only speculate that the Kapitza number, $\mu_f^4 g/(\rho\sigma^3)$, suggested by Mudawar and El-Masri [13] and Saibabu *et al.* [14], is one such parameter since it provides some measure of interfacial effects.

Table 2. Summary of the heat transfer coefficient results

Γ (kg m^{-1} s^{-1})	$\bar{q}$ (W m^{-2})	T_{fm} (°C)	Re	Pr	V_w (m s^{-1})	τ_w (s)	λ (m)	$(\Delta T_w)_{max}$ (°C)	$(\Delta T_{fi})_{max}$ (°C)	$\frac{(\Delta T_w)_{max}}{\frac{1}{\lambda}\int_0^{\lambda}(T_w - T_{fm})\,d\zeta}$	$\bar{h}$ (W m^{-2} K^{-1})	$(h/\bar{h})_{min}$	$(h/\bar{h})_{max}$	$\Delta(h/\bar{h})$
0.61	75000	32.6	3200	5.11	1.2	0.16	0.19	0.9	7.3	0.07	5640	0.54	1.33	0.79
0.61	50000	29.0	3000	5.57	1.2	0.16	0.19	0.4	3.6	0.04	5420	0.76	1.27	0.51
0.61	25000	28.5	3000	5.64	1.2	0.23	0.27	0.3	2.3	0.08	5300	0.58	1.30	0.72
0.61	10000	28.5	3000	5.64	1.2	0.14	0.17	0.1	1.1	0.07	5080	0.48	1.46	0.98
1.22	75000	31.0	6300	5.30	1.8	0.19	0.35	0.5	3.3	0.05	7410	0.71	1.17	0.46
1.22	50000	25.6	5600	6.05	1.8	0.13	0.23	0.2	1.7	0.03	6670	0.81	1.13	0.32
1.22	25000	23.8	5300	6.35	1.8	0.12	0.22	0.1	1.2	0.04	6240	0.75	1.18	0.43
1.22	10000	24.7	5400	6.21	1.8	0.10	0.18	0.1	0.6	0.03	5820	0.74	1.22	0.48
2.44	75000	28.1	11700	5.70	2.2	0.08	0.19	0.1	0.9	0.01	9080	0.92	1.06	0.14
2.44	50000	24.6	10800	6.22	2.2	0.09	0.19	0.1	0.8	0.01	8410	0.90	1.06	0.16
2.44	25000	21.1	10000	6.82	2.2	0.08	0.17	0.1	0.5	0.01	7550	0.89	1.11	0.22
2.44	10000	24.2	10700	6.28	2.2	0.10	0.22	0.1	0.4	0.04	7480	0.73	1.23	0.50

7. SUMMARY

The present study provides a new procedure for determining the wall temperature and convection heat transfer coefficient in a wavy falling liquid film sub-

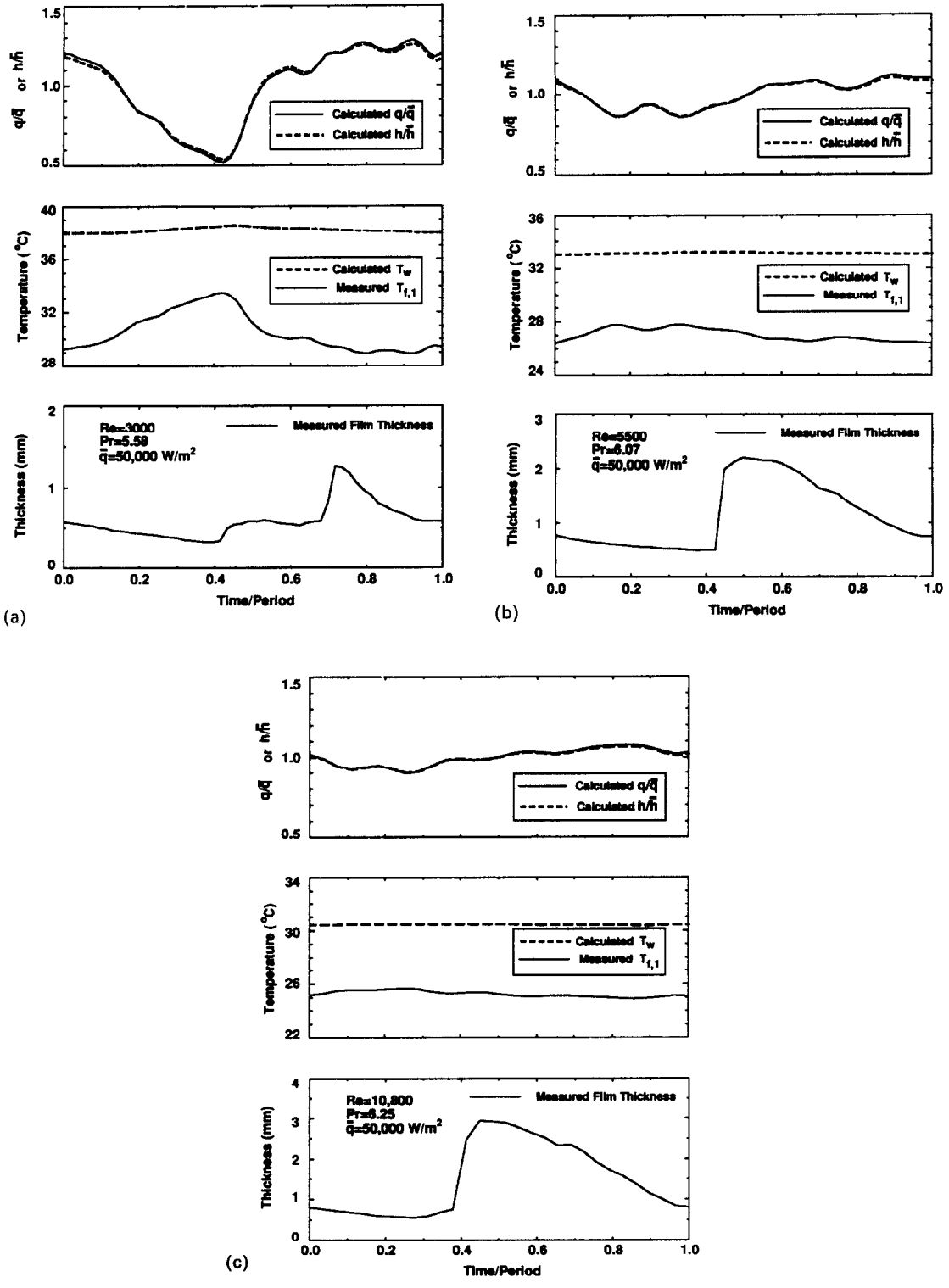

FIG. 10. Variations of wall temperature, wall heat flux and convection heat transfer coefficient during a wave period for: (a) $Re = 3000$; (b) $Re = 5500$; (c) $Re = 10\,800$.

jected to sensible heating. The procedure consists of decomposing the wall temperature into a steady component, which increases with stream-wise distance, and a periodic component, followed by transforming the stationary coordinate system into a moving one. This yields a steady-state energy equation which can be easily solved numerically using liquid temperature measurements in defining the wall–liquid interfacial boundary conditions.

Results show that the wall temperature is fairly

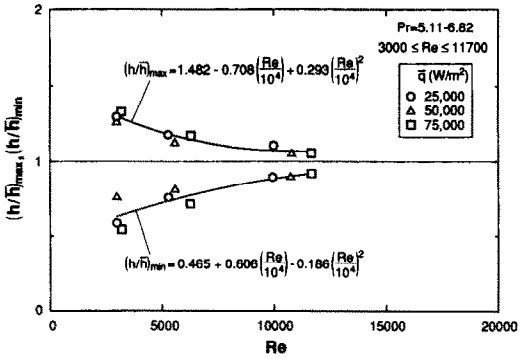

FIG. 11. Variations of $(h/\bar{h})_{max}$ and $(h/\bar{h})_{min}$ with Re.

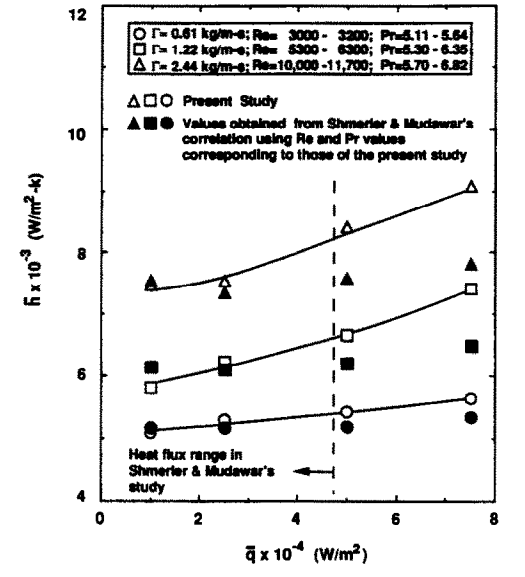

FIG. 12. Effect of heat flux on the convection heat transfer coefficient for fixed values of Re and Pr_f.

steady, insensitive to the passage of large waves for most conditions, due to the high speeds of typical film waves. Also shown are the significant variations in the convection heat transfer coefficient over a wave period for $Re \lesssim 3000$ and the relatively weaker variations for $Re \gtrsim 10\,000$. It is also revealed that correlations based upon the Reynolds and Prandtl numbers alone may not be accurate in predicting the time average heat transfer coefficient at high heat flux due to the strong coupled effects of heat transfer and interfacial waviness at these conditions.

Acknowledgement—This paper is based upon work partially supported by the U.S. Department of Energy, Office of Basic Energy Sciences through Grant No. DE-85ER13398.

REFERENCES

1. A. E. Dukler, Characterization, effects and modelling of the wavy gas–liquid interface. In *Progress in Heat and Mass Transfer*, Vol. 6, pp. 207–234. Pergamon Press, New York (1972).
2. M. Miya, D. Woodmansee and T. J. Hanratty, A model for roll waves in gas–liquid flow, *Chem. Engng Sci.* **26**, 1915–1931 (1971).
3. N. Brauner and D. M. Maron, Characteristics of inclined thin films, waviness and the associated mass transfer, *Int. J. Heat Mass Transfer* **25**, 99–110 (1982).
4. B. G. Ganchev and V. V. Trishin, Fluctuation of wall temperature in film cooling, *Fluid Mech.—Sov. Res.* **16**, 17–23 (1987).
5. J. A. Shmerler and I. Mudawar, Local heat transfer coefficient in wavy free-falling turbulent liquid films undergoing uniform sensible heating, *Int. J. Heat Mass Transfer* **31**, 67–77 (1988).
6. T. H. Lyu and I. Mudawar, Statistical investigation of the relationship between interfacial waviness and heat transfer to a falling liquid film, *Int. J. Heat Mass Transfer* **34**, 1451–1464 (1991).
7. K. J. Chu and A. E. Dukler, Statistical characteristics of thin, wavy films, part III. Structure of the large waves and their resistance to gas flow, *A.I.Ch.E. Jl* **21**, 583–593 (1975).
8. H. Takahama and S. Kato, Longitudinal flow characteristics of vertically falling liquid films without concurrent gas flow, *Int. J. Multiphase Flow* **6**, 203–215 (1980).
9. S. V. Patankar, *Numerical Heat Transfer and Fluid Flow*. Hemisphere, Washington, DC (1980).
10. W. J. Marsh and I. Mudawar, Predicting the onset of nucleate boiling in wavy free-falling turbulent liquid films, *Int. J. Heat Mass Transfer* **32**, 361–378 (1989).
11. A. Faghri and R. A. Seban, Heat transfer in wavy liquid films, *Int. J. Heat Mass Transfer* **28**, 506–508 (1985).
12. F. K. Wasden and A. E. Dukler, Insights into the hydrodynamics of free falling wavy films, *A.I.Ch.E. Jl* **35**, 187–195 (1989).
13. I. Mudawar and M. A. El-Masri, Momentum and heat transfer across freely-falling turbulent liquid films, *Int. J. Multiphase Flow* **12**, 771–790 (1986).
14. J. Saibabu, P. K. Sarma, V. D. Rao and G. J. V. J. Raju, Experimental and theoretical investigation on dynamics and heating of turbulent falling films, *Proc. 8th Int. Heat Transfer Conf.*, San Francisco, Vol. 4, pp. 1963–1969 (1986).

DETERMINATION DES FLUCTUATIONS DE TEMPERATURE PARIETALE INDUITES PAR LES ONDULATIONS ET COEFFICIENT DE CONVECTION THERMIQUE DANS LE CHAUFFAGE D'UN FILM LIQUIDE TOMBANT ET TURBULENT

Résumé—On étudie la réponse thermique variable d'une paroi verticale chauffée électriquement pendant le chauffage d'un film turbulent. On montre que la température de la paroi peut être décomposée en deux termes. Le premier est permanent et rend compte de l'accroissement, dans le sens de l'écoulement, des températures de la paroi et du film, et le second, périodique, correspond aux fluctuations de température dues aux ondulations du film. En supposant la périodicité de la fluctuation de la température pariétale en réponse aux grandes ondulations du film, le second terme est résolu numériquement en utilisant des données de température de liquide mesurée à travers le film pour définir la condition limite à l'interface paroi–liquide. Les résultats montrent que, pendant la période d'une grande ondulation, la température pariétale est à peu près uniforme mais le coefficient de convection subit une fluctuation significative. L'amplitude de la fluctuation décroît quand le nombre de Reynolds du film augmente.

BESTIMMUNG VON SCHWANKUNGEN DER WANDTEMPERATUR UND DES WÄRMEÜBERGANGSKOEFFIZIENTEN, HERVORGERUFEN DURCH WELLEN IN EINEM BEHEIZTEN, TURBULENTEN, FALLENDEN FLÜSSIGKEITSFILM

Zusammenfassung—Das instationäre thermische Verhalten einer senkrechten, elektrisch beheizten Wand bei der sensiblen Erwärmung eines turbulenten, welligen Films wird untersucht. Es wird gezeigt, daß die Wandtemperatur in zwei Komponenten aufgespalten werden kann. Die erste Komponente ist zeitlich konstant und repräsentiert die Erhöhung der Film- und Wandtemperatur in Strömungsrichtung. Die zweite ist periodisch und entspricht den Schwankungen der Wandtemperatur infolge der Filmwelligkeit. Unter der Annahme, daß die Schwankungen der Wandtemperatur infolge der großen Wellen im Film periodisch sind, wird die zweite Komponente der Wandtemperatur numerisch bestimmt. Dabei wird die gemessene Temperaturverteilung im Film quer zur Strömungsrichtung verwendet, um die Randbedingungen an der Wandoberfläche zu bestimmen. Die Ergebnisse zeigen, daß während einer Periode einer großen Welle die Wandtemperatur annähernd konstant bleibt, der Wärmeübergangskoeffizient dagegen deutlichen Schwankungen unterworfen ist. Die Amplitude der Schwankungen nimmt mit steigender Film-Reynolds-Zahl ab.

ОПРЕДЕЛЕНИЕ ФЛУКТУАЦИЙ ТЕМПЕРАТУРЫ СТЕНКИ И КОЭФФИЦИЕНТА КОНВЕКТИВНОГО ТЕПЛОПЕРЕНОСА ПРИ НАГРЕВЕ ТУРБУЛЕНТНОЙ СТЕКАЮЩЕЙ ЖИДКОЙ ПЛЕНКИ ПРИ НАЛИЧИИ ВОЛН НА ПОВЕРХНОСТИ

Аннотация—Исследуется нестационарный тепловой откцик вертикальной стенки, нагреваемой электрическим током и вызывающей нагрев стекающей турбулентной волнистой пленки. Дается способ разделения температуры стенки на два компонента. Первый является стационарным и учитывает увеличение температур стенки и пленки в направлении течения, второй—периодический и соответствует температурным флуктуациям, обусловленным волнистостью пленки. С целью определения граничного условия на границе раздела стенка—жидкость на основе данных по температуре жидкости, измеряемой в поперечном направлении пленки, численно определяется второй компонент в предположении периодичности флуктуаций температуры стенки за счет больших волн пленки. Полученные результаты показывают, что в течение периода большой волны температура стенки является практически постоянной, в то время как коэффициент конвективного теплопереноса претерпевает существенную флуктуацию, амплитуда которой уменьшается с увеличением числа Рейнольдса для пленки.